Physics Letters B 762 (2016) 253–262

Contents lists available at ScienceDirect

Physics Letters B

www.elsevier.com/locate/physletb

First study of the *CP*-violating phase and decay-width difference in $B_s^0 \to \psi(2S)\phi$ decays

The LHCb Collaboration

ARTICLE INFO

Article history:
Received 17 August 2016
Received in revised form 5 September 2016
Accepted 15 September 2016
Available online 20 September 2016
Editor: M. Doser

ABSTRACT

A time-dependent angular analysis of $B_s^0 \to \psi(2S)\phi$ decays is performed using data recorded by the LHCb experiment. The data set corresponds to an integrated luminosity of $3.0\,\text{fb}^{-1}$ collected during Run 1 of the LHC. The *CP*-violating phase and decay-width difference of the B_s^0 system are measured to be $\phi_s = 0.23^{+0.29}_{-0.28} \pm 0.02\,\text{rad}$ and $\Delta\Gamma_s = 0.066^{+0.041}_{-0.044} \pm 0.007\,\text{ps}^{-1}$, respectively, where the first uncertainty is statistical and the second systematic. This is the first time that ϕ_s and $\Delta\Gamma_s$ have been measured in a decay containing the $\psi(2S)$ resonance.

1. Introduction

The interference between the amplitudes of decays of B_s^0 mesons to $c\bar{c}X$ *CP* eigenstates directly or via mixing, gives rise to a *CP*-violating phase, ϕ_s. In the Standard Model (SM), ignoring subleading penguin contributions, this phase is predicted to be $-2\beta_s$, where $\beta_s = \arg[-(V_{ts}V_{tb}^*)/(V_{cs}V_{cb}^*)]$ and V_{ij} are elements of the CKM quark flavour mixing matrix [1].

Measurements of ϕ_s using $B_s^0 \to J/\psi K^+K^-$ and $B_s^0 \to J/\psi\pi^+\pi^-$ decays have been reported previously by the LHCb collaboration [2] based upon $3.0\,\text{fb}^{-1}$ of integrated luminosity collected in *pp* collisions at a centre-of-mass energy of 7 TeV in 2011 and 8 TeV in 2012 at the LHC. Measurements of ϕ_s using $B_s^0 \to J/\psi\phi$ decays have also been made by the D0 [3], CDF [4], CMS [5] and ATLAS [6] collaborations. The world-average value of these direct measurements is $\phi_s = -0.033 \pm 0.033\,\text{rad}$ [7]. The global average from indirect measurements gives $\phi_s = -0.0376^{+0.0007}_{-0.0008}$ rad [8]. Measurements of ϕ_s are interesting since new physics (NP) processes could modify the phase if new particles were to contribute to the box diagrams describing B_s^0–$\overline{B}_s^0$ mixing [9,10].

In this analysis ϕ_s is measured using a flavour tagged, decay-time dependent angular analysis of $B_s^0 \to \psi(2S)\phi$ decays, with $\psi(2S) \to \mu^+\mu^-$ and $\phi \to K^+K^-$. In addition, measurements of the decay-width difference of the light (L) and heavy (H) B_s^0 mass eigenstates, $\Delta\Gamma_s \equiv \Gamma_\text{L} - \Gamma_\text{H}$, the average B_s^0 decay width, $\Gamma_s \equiv (\Gamma_\text{L} + \Gamma_\text{H})/2$, and the polarisation amplitudes of the $B_s^0 \to \psi(2S)\phi$ decay are reported. This is the first time that a higher $c\bar{c}$ resonance is used to measure ϕ_s.

This analysis follows very closely that of $B_s^0 \to J/\psi K^+K^-$ decays in Refs. [2,11], and only significant changes with respect to those analyses are described in this paper. Section 2 describes the phenomenology of the $B_s^0 \to \psi(2S)\phi$ decay and the physics observables. Section 3 describes the LHCb detector, data and simulated samples that are used along with the optimisation of their selection. Section 4 details the B_s^0 meson decay-time resolution, decay-time efficiency and angular acceptance and Section 5 describes the flavour tagging algorithms. Results and systematic uncertainties are given in Section 6 and Section 7, respectively. Conclusions are presented in Section 8.

2. Phenomenology

The full formalism used for this analysis can be found in Ref. [11], where the J/ψ is now replaced with the $\psi(2S)$ meson. The differential cross-section as a function of the signal decay time, t, and three helicity angles, $\Omega = (\cos\theta_\mu, \cos\theta_K, \varphi)$ (Fig. 1), is described by a sum of ten terms, corresponding to the four polarisation amplitudes (three corresponding to the K^+K^- from the ϕ being in a P-wave configuration, and one to allow for an additional non-resonant K^+K^- S-wave component) and their interference terms. Each term is the product of a time-dependent function and an angular function,

$$X(t,\Omega) \equiv \frac{\mathrm{d}^4\Gamma(B_s^0 \to \psi(2S)\phi)}{\mathrm{d}t\,\mathrm{d}\Omega} \propto \sum_{k=1}^{10} h_k(t)\, f_k(\Omega)\,, \tag{1}$$

where the definitions of $h_k(t)$ and $f_k(\Omega)$ are given in Ref. [11]. The $f_k(\Omega)$ functions depend only upon the final-state decay angles. The $h_k(t)$ functions depend upon all physics parameters of interest, which are Γ_s, $\Delta\Gamma_s$, ϕ_s, $|\lambda|$, the mass difference of the B_s^0 eigenstates, Δm_s, and the polarisation amplitudes $A_i = |A_i|e^{-i\delta_i}$, where the indices $i \in \{0, \parallel, \perp, S\}$ refer to the different polarisation states of the K^+K^- system. The sum $|A_\parallel|^2 + |A_0|^2 + |A_\perp|^2$ equals

http://dx.doi.org/10.1016/j.physletb.2016.09.028

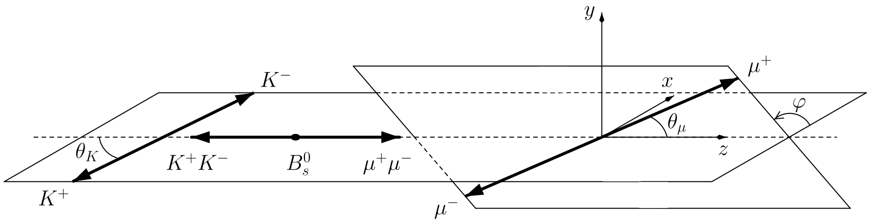

Fig. 1. Definition of helicity angles.

unity and by convention δ_0 is zero. The S-wave fraction is defined as $F_S \equiv |A_S|^2/(|A_0|^2 + |A_\perp|^2 + |A_\parallel|^2 + |A_S|^2)$. The parameter λ describes *CP* violation in the interference between mixing and decay and is defined by $\lambda = \eta_i (q/p)(\bar{A}_i/A_i)$. The complex parameters $p = \langle B_s^0 | B_{s,\mathrm{L}} \rangle$ and $q = \langle \overline{B}_s^0 | B_{s,\mathrm{L}} \rangle$ describe the relation between flavour and mass eigenstates, where $B_{s,\mathrm{L}}$ is the light mass eigenstate and η_i is the *CP* eigenvalue of the polarisation state i. The *CP*-violating phase is defined by $\phi_s \equiv -\arg(\eta_i \lambda)$ and is assumed here to be the same for all polarisation states. In the absence of *CP* violation in decay it follows that $|\lambda| = 1$. In this paper *CP* violation in B_s^0-meson mixing is assumed to be negligible, following measurements in Refs. [12,13].

3. Detector, data set and selection

The LHCb detector [14,15] is a single-arm forward spectrometer covering the pseudorapidity range $2 < \eta < 5$, designed for the study of particles containing b or c quarks. The detector includes a high-precision tracking system consisting of a silicon-strip vertex detector surrounding the pp interaction region, a large-area silicon-strip detector located upstream of a dipole magnet with a bending power of about 4 Tm, and three stations of silicon-strip detectors and straw drift tubes placed downstream of the magnet. The tracking system provides a measurement of momentum, p, of charged particles with a relative uncertainty that varies from 0.5% at low momentum to 1.0% at 200 GeV/c. The minimum distance of a track to a primary vertex (PV), the impact parameter, is measured with a resolution of $(15 + 29/p_\mathrm{T})\,\mu\mathrm{m}$, where p_T is the component of the momentum transverse to the beam, in GeV/c. Different types of charged hadrons are distinguished using information from two ring-imaging Cherenkov detectors. Photons, electrons and hadrons are identified by a calorimeter system consisting of scintillating-pad and preshower detectors, an electromagnetic calorimeter and a hadronic calorimeter. Muons are identified by a system composed of alternating layers of iron and multiwire proportional chambers.

The online event selection is performed by a trigger [16], which consists of a hardware stage, based on information from the calorimeter and the muon system, followed by a software stage. In this analysis, candidates are required to pass the hardware trigger that selects muons and muon pairs based on their transverse momentum. In the software stage, events are triggered by a $\psi(2S) \to \mu^+\mu^-$ candidate, where the $\psi(2S)$ is required to be consistent with coming from the decay of a b hadron, by using either impact parameter requirements on the decay products or the detachment of the $\psi(2S)$ candidate from the PV.

In the simulation, pp collisions are generated using Pythia [17] with a specific LHCb configuration [18]. Decays of hadronic particles are described by EvtGen [19], in which final-state radiation is generated using Photos [20]. The interaction of the generated particles with the detector, and its response, are implemented using the Geant4 toolkit [21] as described in Ref. [22].

The $B_s^0 \to \psi(2S)\phi$ candidates are first selected with loose requirements to ensure high efficiency and significant background rejection. The $\psi(2S)$ candidates are reconstructed from pairs of oppositely-charged particles identified as muons, and the ϕ candidates are reconstructed from pairs of oppositely-charged particles identified as kaons. The invariant mass of the muon (kaon) pair must be within 60 MeV/c^2 (12 MeV/c^2) of the known $\psi(2S)$ (ϕ) mass [23]. Reconstructed kaon tracks that do not correspond to actual trajectories of charged particles are suppressed by requiring a good track χ^2 per degree of freedom. The p_T of each ϕ candidate is required to be larger than 1 GeV/c.

The $\psi(2S)$ and ϕ candidates that are consistent with originating from a common vertex are combined to create B_s^0 candidates. Subsequently, a kinematic fit [24] is applied to the B_s^0 candidates in which the $\psi(2S)$ mass is constrained to the known value [23] and the B_s^0 candidate is required to point back to the PV, to improve the resolution on the invariant mass $m(\psi(2S)K^+K^-)$. Combinatorial background from particles produced at the PV is reduced by requiring that the B_s^0 candidate decay time (computed from a vertex fit without the PV constraint) is larger than 0.3 ps. Backgrounds from the misidentification of final-state particles from other decays such as $B^0 \to \psi(2S)K^+\pi^-$ and $\Lambda_b^0 \to \psi(2S)pK^-$ are negligible.

To further improve the signal-to-background ratio, a boosted decision tree (BDT) [25,26] is applied. The BDT is trained using simulated $B_s^0 \to \psi(2S)\phi$ events for the signal, while candidates from data with $m(\psi(2S)K^+K^-)$ larger than 5400 MeV/c^2 are used to model the background. Twelve variables that have good discrimination power between signal and background are used to define and train the BDT. These are: the B_s^0 candidate kinematic fit χ^2; the p_T of the B_s^0 and ϕ candidates; the B_s^0 candidate flight distance and impact parameter with respect to the PV; the $\psi(2S)$ candidate vertex χ^2; the χ^2_IP of the kaon and muon candidates (defined as the change in χ^2 of the PV fit when reconstructed with and without the considered particle) and the muon identification probabilities. The optimal working point for the BDT is determined using a figure of merit that optimises the statistical power of the selected data sample for the analysis of ϕ_s by taking account of the number of signal and background candidates, as well as the decay-time resolution and flavour-tagging power of each candidate.

Fig. 2 shows the distribution of $m(\psi(2S)K^+K^-)$ for the selected $B_s^0 \to \psi(2S)\phi$ candidates. An extended maximum likelihood fit is made to the unbinned $m(\psi(2S)K^+K^-)$ distribution, where the signal component is described by the sum of two Crystal Ball [27] functions and the small combinatorial background by an exponential function. All parameters are left free in the fit, including the yields of the signal and background components. This fit gives a yield of 4695 ± 71 signal candidates and 174 ± 10 background candidates in the range $m(\psi(2S)K^+K^-) \in [5310, 5430]\,\mathrm{MeV}/c^2$. It is used to assign per-candidate weights (sWeights) via the sPlot technique [28], which are used to subtract the background contribution in the maximum likelihood fit described in Section 6.

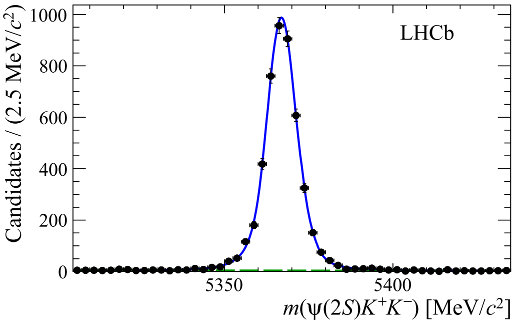

Fig. 2. Distribution of $m(\psi(2S)K^+K^-)$ for the selected $B_s^0 \to \psi(2S)\phi$ candidates. The total fit model is shown by the solid blue line, which is composed of a sum of two Crystal Ball functions for the signal and an exponential function for the background (long-dashed green line). (For interpretation of the references to colour in this figure legend, the reader is referred to the web version of this article.)

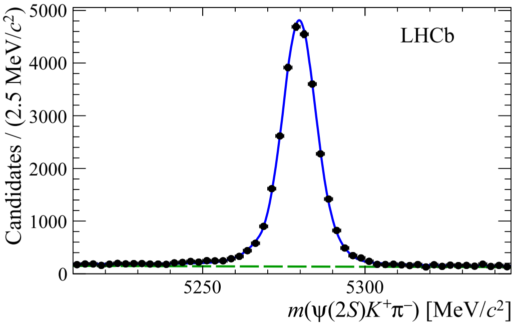

Fig. 3. Distribution of $m(\psi(2S)K^+\pi^-)$ of the selected $B^0 \to \psi(2S)K^*(892)^0$ candidates. The total fit model is shown by the solid blue line, which is composed of a sum of two Crystal Ball functions for the signal and an exponential function for the background (long-dashed green line). (For interpretation of the references to colour in this figure legend, the reader is referred to the web version of this article.)

4. Detector resolution and efficiency

The resolution on the measured decay time is determined with the same method as described in Refs. [2,11] by using a large sample of prompt $J/\psi K^+K^-$ combinations produced directly in the pp interactions. These events are selected using prompt $J/\psi \to \mu^+\mu^-$ decays via a prescaled trigger that does not impose any requirements on the separation of the J/ψ from the PV. The J/ψ candidates are combined with oppositely charged tracks that are identified as kaons, using a similar selection as for the signal decay. The resolution model, $R(t-t')$, is the sum of two Gaussian distributions with per-event widths. These widths are calibrated by using a maximum likelihood fit to the unbinned decay time and decay-time uncertainty distributions of the prompt $J/\psi K^+K^-$ combinations, using a model composed of the sum of a δ function for the prompt component and two exponential functions for long-lived backgrounds, all of which are convolved with the resolution function. A third Gaussian distribution is added to the total fit function to account for the small ($< 1\%$) fraction of decays that are associated to the wrong PV. The average effective resolution is 46.6 ± 1.0 fs. Simulated $B_s^0 \to J/\psi K^+K^-$ and $B_s^0 \to \psi(2S)K^+K^-$ events show no significant difference in the effective decay-time resolution between the two decay modes.

The reconstruction efficiency is not constant as a function of decay time due to displacement requirements made on signal tracks in the trigger and event selection. The efficiency is determined using the control channel $B^0 \to \psi(2S)K^*(892)^0$, with $K^*(892)^0 \to K^+\pi^-$, which is assumed to have a purely exponential decay-time distribution. It is defined as

$$\varepsilon^{B_s^0}_{\rm data}(t) = \varepsilon^{B^0}_{\rm data}(t) \times \frac{\varepsilon^{B_s^0}_{\rm sim}(t)}{\varepsilon^{B^0}_{\rm sim}(t)}, \tag{2}$$

where $\varepsilon^{B^0}_{\rm data}(t)$ is the efficiency of the control channel and $\varepsilon^{B_s^0}_{\rm sim}(t)/\varepsilon^{B^0}_{\rm sim}(t)$ is the ratio of efficiencies of the simulated signal and control modes after the full trigger and selection chain has been applied. This correction accounts for the small differences in the lifetime and kinematics between the signal and control modes.

The $B^0 \to \psi(2S)K^*(892)^0$ decay is selected using a similar trigger, preselection and the same BDT training and working point as used for the signal (with appropriate changes for kaon to pion). Backgrounds from the misidentification of final-state particles from other decays such as $B_s^0 \to \psi(2S)\phi$ and $\Lambda_b^0 \to \psi(2S)pK^-$ are negligible. Similarly, possible backgrounds from $B^0_{(s)} \to \psi(2S)\pi^+\pi^-$ decays where a pion is misidentified as a kaon, and $B^+ \to \psi(2S)K^+$ decays combined with an additional random pion, are negligible.

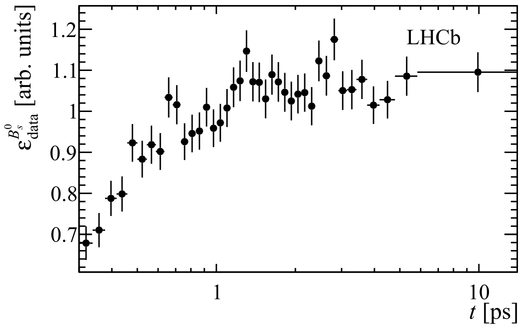

Fig. 4. Decay-time efficiency $\varepsilon^{B_s^0}_{\rm data}(t)$ in arbitrary units.

The $\psi(2S)K^+\pi^-$ invariant mass distribution is shown in Fig. 3 along with the result of a fit composed of the sum of two Crystal Ball (CB) functions for the signal and an exponential function for the background. The tail parameters and relative fraction of the two CB functions are fixed to values obtained from a fit to simulated $B^0 \to \psi(2S)K^*(892)^0$ decays. The core widths and common mean of the CB functions are free in the fit and the B^0 yield is found to be $28\,676 \pm 195$. The efficiency is defined as $\varepsilon^{B^0}_{\rm data}(t) = N^{B^0}_{\rm data}(t)/N^{B^0}_{\rm gen}(t)$ where $N^{B^0}_{\rm data}(t)$ is the number of signal $B^0 \to \psi(2S)K^*(892)^0$ decays in a given bin of decay time and $N^{B^0}_{\rm gen}(t)$ is the number of events generated from an exponential distribution with lifetime $\tau_{B^0} = 1.520 \pm 0.004$ ps [23]. The exponential distribution is convolved with a double Gaussian resolution model, the parameters of which are determined from a fit to the decay time distribution of prompt $J/\psi K^+\pi^-$ combinations. In total 10^7 events are generated. The sPlot [28] technique with $m(\psi(2S)K^+\pi^-)$ as discriminating variable is used to determine $N^{B^0}_{\rm data}(t)$. The analysis is not sensitive to the absolute scale of the efficiency. The final decay-time efficiency for the $B_s^0 \to \psi(2S)\phi$ signal is shown in Fig. 4. It is relatively uniform at high values of decay time but decreases at low decay times due to selection requirements placed on the track $\chi^2_{\rm IP}$ variables.

The efficiency as a function of the $B_s^0 \to \psi(2S)\phi$ helicity angles is not uniform due to the forward geometry of the LHCb detector and the requirements imposed on the final-state particle momenta. The three-dimensional efficiency, $\varepsilon(\Omega)$, is determined with the same technique as used in Ref. [11] using simulated events that are subjected to the same trigger and selection criteria as the data. The relative efficiencies vary by up to 20%, dominated by the dependence on $\cos\theta_\mu$.

5. Flavour tagging

The B_s^0 candidate flavour at production is determined by two independent classes of flavour tagging algorithms, the opposite-side (OS) taggers [29] and the same-side kaon (SSK) tagger [30], which exploit specific features of the production of $b\bar{b}$ quark pairs in pp collisions, and their subsequent hadronisation. Each tagging algorithm gives a tag decision and a mistag probability. The tag decision, q, takes values +1, −1, or 0, if the signal meson is tagged as B_s^0, $\overline{B}{}_s^0$, or is untagged, respectively. The fraction of events in the sample with a nonzero tagging decision gives the efficiency of the tagger, $\varepsilon_{\rm tag}$. The mistag probability, η, is estimated event-by-event, and represents the probability that the algorithm assigns a wrong tag decision to the event; it is calibrated using data samples of several flavour-specific B^0, B^+ and B_{s2}^{*0} decays to obtain the corrected mistag probability, $\overset{(-)}{\omega}$, for an initial flavour $\overset{(-)}{B}{}_s^0$meson. A linear relationship between η and $\overset{(-)}{\omega}$ is used for the calibration. The effective tagging power is given by $\varepsilon_{\rm tag}(1-2\omega)^2$ and for the combined taggers in the $B_s^0 \to \psi(2S)\phi$ signal sample is $(3.88 \pm 0.13 \pm 0.12)\%$, where the first uncertainty is statistical and the second systematic.

6. Maximum likelihood fit

The physics parameters are determined by a weighted maximum likelihood fit of a signal-only probability density function (PDF) to the four-dimensional distribution of $B_s^0 \to \psi(2S)\phi$ decay time and helicity angles. The negative log-likelihood function to be minimised is given by

$$-\ln\mathcal{L} = -\alpha \sum_{\text{events } i} W_i \ln\mathcal{P}, \tag{3}$$

where W_i are the sWeights computed using $m(\psi(2S)K^+K^-)$ as the discriminating variable and the factor $\alpha = \sum W_i / \sum W_i^2$ is necessary to obtain the correct parameter uncertainties from the Hessian of the negative log-likelihood. The PDF, $\mathcal{P} = \mathcal{S}/\int \mathcal{S}\,\mathrm{d}t\,\mathrm{d}\Omega$, is obtained from

$$\mathcal{S}(t,\Omega,\mathrm{q}^{\rm OS},\mathrm{q}^{\rm SSK}|\eta^{\rm OS},\eta^{\rm SSK}) = \mathcal{X}(t',\Omega,\mathrm{q}^{\rm OS},\mathrm{q}^{\rm SSK}|\eta^{\rm OS},\eta^{\rm SSK}) \otimes R(t-t') \times \varepsilon_{\rm data}^{B_s^0}(t), \tag{4}$$

where

$$\begin{aligned}\mathcal{X}(t,\Omega,&\mathrm{q}^{\rm OS},\mathrm{q}^{\rm SSK}|\eta^{\rm OS},\eta^{\rm SSK})\\ &= \left(1+\mathrm{q}^{\rm OS}(1-2\omega^{\rm OS})\right)\left(1+\mathrm{q}^{\rm SSK}(1-2\omega^{\rm SSK})\right)X(t,\Omega)\\ &\quad + \left(1-\mathrm{q}^{\rm OS}(1-2\bar{\omega}^{\rm OS})\right)\left(1-\mathrm{q}^{\rm SSK}(1-2\bar{\omega}^{\rm SSK})\right)\overline{X}(t,\Omega),\end{aligned} \tag{5}$$

which allows for the inclusion of information from both tagging algorithms in the computation of the decay rate. The function $X(t,\Omega)$ is defined in Eq. (1) and $\overline{X}(t,\Omega)$ is the corresponding function for $\overline{B}{}_s^0$ decays. As in Ref. [11], the angular efficiency is included in the normalisation of the PDF via ten integrals, $I_k = \int \mathrm{d}\Omega\,\varepsilon(\Omega)\,f_k(\Omega)$, which are calculated using simulated events. In contrast to Refs. [2,11], the fit is performed in a single bin of $m(K^+K^-)$, within $12\,\mathrm{MeV}/c^2$ of the known ϕ mass.

Table 1
Results of the maximum likelihood fit to the selected $B_s^0 \to \psi(2S)\phi$ candidates including all acceptance and resolution effects. The first uncertainty is statistical and the second is systematic, which will be discussed in Section 7.

Parameter	Value
Γ_s [ps^{-1}]	$0.668 \pm 0.011 \pm 0.006$
$\Delta\Gamma_s$ [ps^{-1}]	$0.066^{+0.041}_{-0.044} \pm 0.007$
$\lvert A_\perp\rvert^2$	$0.264^{+0.024}_{-0.023} \pm 0.002$
$\lvert A_0\rvert^2$	$0.422 \pm 0.014 \pm 0.003$
$\delta_\parallel$ [rad]	$3.67^{+0.13}_{-0.18} \pm 0.03$
$\delta_\perp$ [rad]	$3.29^{+0.43}_{-0.39} \pm 0.04$
ϕ_s [rad]	$0.23^{+0.29}_{-0.28} \pm 0.02$
$\lvert\lambda\rvert$	$1.045^{+0.069}_{-0.050} \pm 0.007$
F_S	$0.061^{+0.026}_{-0.025} \pm 0.007$
δ_S [rad]	$0.03 \pm 0.14 \pm 0.02$

In the fit, Gaussian constraints are applied to the B_s^0 mixing frequency $\Delta m_s = 17.757 \pm 0.021\,\mathrm{ps}^{-1}$ [7] and the tagging calibration parameters. The fitting procedure has been validated using pseudoexperiments and simulated $B_s^0 \to \psi(2S)\phi$ decays. Due to the symmetry in the PDF there is a two-fold ambiguity in the solutions for ϕ_s and $\Delta\Gamma_s$; the solution with positive $\Delta\Gamma_s$ is used [31]. The results of the fit to the data are shown in Tables 1 and 2 while the projections of the fit onto the data are shown in Fig. 5. The results are consistent with previous measurements of these parameters [2–6], and the SM predictions for ϕ_s and $\Delta\Gamma_s$ [32–34]. They show no evidence of *CP* violation in the interference between B_s^0 meson mixing and decay, nor for direct *CP* violation in $B_s^0 \to \psi(2S)\phi$ decays as the parameter $|\lambda|$ is consistent with unity. The likelihood profile for $\delta_\parallel$ is not parabolic and the 95% confidence level range is $[2.4, 3.9]$ rad.

Fig. 6 shows values of $F_{\rm L} \equiv |A_0|^2$, the fraction of longitudinal polarisation, for $B_s^0 \to \phi\mu^+\mu^-$ [35], $B_s^0 \to J/\psi\phi$ [2] and $B_s^0 \to \psi(2S)\phi$ final states as a function of the invariant mass squared of the dimuon system, q^2. The precise measurement of $F_{\rm L}$ from $B_s^0 \to J/\psi\phi$ at $q^2 = 9.6\,\mathrm{GeV}^2/c^4$ is now joined by the precise measurement from this paper at $q^2 = 13.6\,\mathrm{GeV}^2/c^4$, demonstrating a clear decrease with q^2 towards the value of 1/3, as predicted by Ref. [36].

7. Systematic uncertainties

Systematic uncertainties for each of the measured parameters are reported in Table 3. They are evaluated by observing the change in physics parameters after repeating the likelihood fit with a modified model assumption, or by generating pseudoexperiments

Table 2
Correlation matrix of statistical uncertainties.

	Γ_s	$\Delta\Gamma_s$	$\lvert A_\perp\rvert^2$	$\lvert A_0\rvert^2$	$\delta_\parallel$	$\delta_\perp$	F_S	δ_S	ϕ_s	$\lvert\lambda\rvert$
Γ_s	1.00	−0.40	0.35	−0.27	−0.08	−0.02	0.15	0.02	0.02	−0.04
$\Delta\Gamma_s$		1.00	−0.66	0.60	0.02	−0.04	−0.10	−0.02	0.19	0.03
$\lvert A_\perp\rvert^2$			1.00	−0.54	−0.31	−0.05	0.08	0.03	−0.02	−0.02
$\lvert A_0\rvert^2$				1.00	0.05	−0.02	−0.15	−0.02	0.07	0.03
$\delta_\parallel$					1.00	0.26	−0.26	−0.01	0.00	0.08
$\delta_\perp$						1.00	−0.21	−0.25	−0.06	0.59
F_S							1.00	0.02	0.05	−0.25
δ_S								1.00	0.07	−0.09
ϕ_s									1.00	0.04
$\lvert\lambda\rvert$										1.00

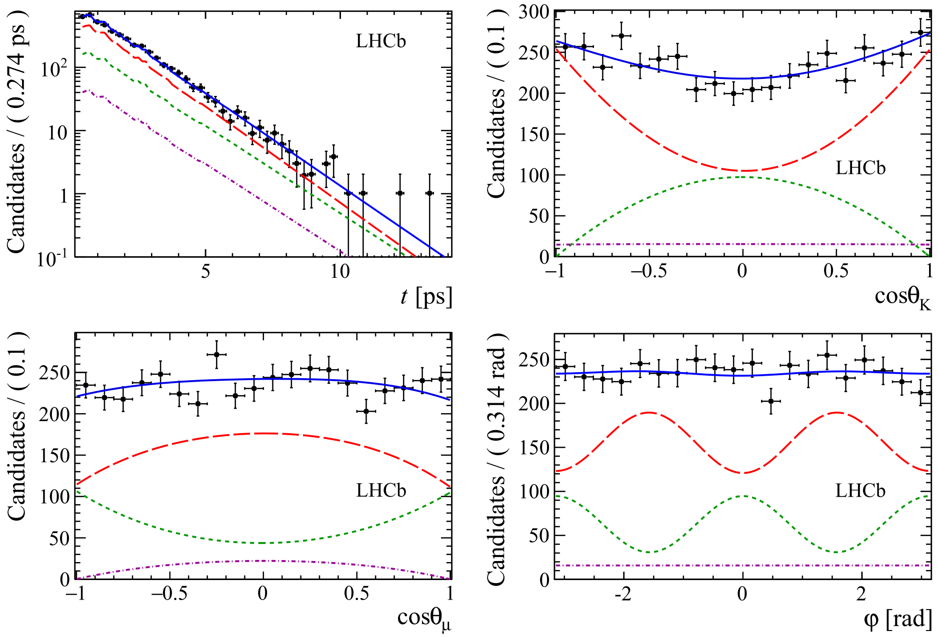

Fig. 5. Decay-time and helicity-angle distributions for $B_s^0 \to \psi(2S)\phi$ decays (data points) with the one-dimensional projections of the fitted PDF. The solid blue line shows the total signal contribution, which is composed of *CP*-even (long-dashed red), *CP*-odd (short-dashed green) and *S*-wave (dash-dotted purple) contributions. (For interpretation of the references to colour in this figure legend, the reader is referred to the web version of this article.)

Table 3
Summary of statistical and systematic uncertainties. Fields containing a dash (–) correspond to systematic uncertainties that are negligible.

Source	Γ_s [ps^{-1}]	$\Delta\Gamma_s$ [ps^{-1}]	$\|A_\perp\|^2$	$\|A_0\|^2$	$\delta_\parallel$ [rad]	$\delta_\perp$ [rad]	ϕ_s [rad]	$\|\lambda\|$	F_S	δ_S [rad]
Stat. uncertainty	0.011	${}^{+0.041}_{-0.044}$	${}^{+0.024}_{-0.023}$	0.014	${}^{+0.13}_{-0.18}$	${}^{+0.43}_{-0.39}$	${}^{+0.29}_{-0.28}$	${}^{+0.069}_{-0.050}$	${}^{+0.026}_{-0.025}$	0.14
Mass factorisation	0.003	0.002	0.001	0.001	0.02	–	0.01	0.001	0.003	0.01
Mass model	0.001	0.001	–	–	–	–	–	0.001	–	–
Angular eff. (stat.)	–	0.001	0.001	0.002	0.02	0.03	0.01	0.006	0.005	0.02
Angular resolution	–	–	0.001	–	0.01	0.01	–	–	–	–
Time resolution	–	0.001	–	–	–	0.02	0.02	0.002	0.002	–
Time resolution (stat.)	–	–	–	–	–	0.02	–	0.002	–	–
Time eff. (stat.)	0.005	0.003	0.001	0.001	–	–	–	–	0.002	–
Time eff. (mass model)	0.001	0.001	–	–	–	–	–	–	–	–
Time eff. (τ_{B^0})	0.002	–	–	–	–	–	–	–	–	–
B_c^+ feed-down	0.001	–	–	–	–	–	–	–	–	–
Fit bias	0.001	0.006	–	0.001	0.01	–	–	–	0.003	–
Quad. sum of syst.	0.006	0.007	0.002	0.003	0.03	0.04	0.02	0.007	0.007	0.02
Total uncertainties	0.013	${}^{+0.042}_{-0.045}$	${}^{+0.024}_{-0.023}$	0.014	${}^{+0.13}_{-0.18}$	${}^{+0.43}_{-0.39}$	${}^{+0.29}_{-0.28}$	${}^{+0.069}_{-0.050}$	${}^{+0.027}_{-0.026}$	0.14

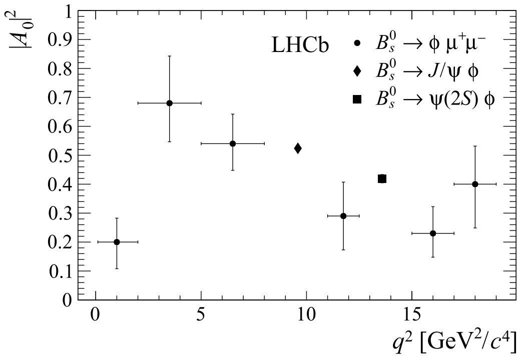

Fig. 6. $|A_0|^2$ as a function of the invariant mass squared of the dimuon system, q^2. Data points are taken from Ref. [35] ($B_s^0 \to \phi\mu^+\mu^-$, circles), Ref. [2] ($B_s^0 \to J/\psi\phi$, diamond) and this paper (square).

in case of uncertainties originating from the limited size of a calibration sample. In general the sum in quadrature of the different sources of systematic uncertainty is less than 20% of the statistical uncertainty, except for Γ_s where it is close to 60%.

Repeating the fit to $m(\psi(2S)K^+K^-)$ in bins of the decay time and helicity angles shows that the mass resolution depends upon $\cos\theta_\mu$. This breaks the assumption that $m(\psi(2S)K^+K^-)$ is uncorrelated with the observables of interest, which is implicitly made by the use of weights from the sPlot technique. The effect of this correlation is quantified by repeating the four-dimensional likelihood fit for different sets of signal weights computed from fits to $m(\psi(2S)K^+K^-)$ in bins of $\cos\theta_\mu$. The largest variation in each physics parameter is assigned a systematic uncertainty. The mass model is tested by computing a new set of sWeights, using a Student's t-function to describe the signal component of the $m(\psi(2S)K^+K^-)$ distribution.

The statistical uncertainty on the angular efficiency is propagated by repeating the fit using new sets of the ten integrals, I_k, systematically varied according to their covariance matrix. The effect of assuming perfect angular resolution in the likelihood fit is studied using pseudoexperiments. There is a small effect on the polarisation amplitudes and strong phases while all other parameters are unaffected.

The decay-time resolution is studied by generating pseudoexperiments using the nominal double Gaussian model and subsequently fitting them using a single Gaussian model, the parameters of which have been calibrated on the prompt $J/\psi K^+K^-$ sample. In addition, the nominal model parameters are varied within their statistical uncertainties and the fit repeated.

The decay-time efficiency introduces a systematic uncertainty from three different sources. First, the contribution due to the statistical error on the determination of the decay-time efficiency from the control channel is determined by repeating the fit multiple times after randomly varying the parameters of the time efficiency within their statistical uncertainties. The statistical uncertainty is dominated by the size of the $B^0 \to \psi(2S)K^*(892)^0$ control sample. Second, a Student's t-function is used as an alternative mass model for the $m(\psi(2S)K^+\pi^-)$ distribution and a new decay-time efficiency function is produced. Finally, the efficiency function is recomputed with the lifetime of the B^0 modified by $\pm 1\sigma$. In all cases the difference in fit results arising from the use of the new efficiency function is taken as a systematic uncertainty. The sensitivity to the BDT selection is studied by adjusting the working point around the optimal position equally for both signal and control channel, and also differently for each channel in order to make the ratio $\varepsilon_{\text{sim}}^{B_s^0}(t)/\varepsilon_{\text{sim}}^{B^0}(t)$ uniform. The efficiency is recomputed in each case and the fit repeated. No significant change in the physics parameters is observed.

A small fraction of $B_s^0 \to \psi(2S)\phi$ signal candidates comes from the decay of B_c^+ mesons, causing an average positive shift in the reconstructed decay time of the B_s^0 meson. This fraction was estimated as 0.8% in Ref. [2] and pseudoexperiments were used to assess the impact of ignoring such a contribution. Only Γ_s was affected, with a bias on its central value of $(+20 \pm 6)\%$ of its statistical uncertainty. The assumption is made that the ratio of efficiencies for selecting $B_s^0 \to \psi(2S)\phi$ decays either promptly or via the decay of B_c^+ mesons is the same as that for $B_s^0 \to J/\psi\phi$ decays. This leads to a bias of $+0.002 \pm 0.001\,\text{ps}^{-1}$ in Γ_s. The central value of Γ_s is therefore reduced by $0.002\,\text{ps}^{-1}$ and a systematic uncertainty of $0.001\,\text{ps}^{-1}$ is assigned.

A test for a possible bias in the fit procedure is performed by generating and fitting many simulated pseudoexperiments of equivalent size to the data sample. The resulting biases are small and those that are not compatible with zero within two standard deviations are quoted as systematic uncertainties.

The uncertainty from knowledge of the LHCb detector's length and momentum scale is negligible as is the statistical uncertainty from the sWeights. The tagging parameters are allowed to float in the fit using Gaussian constraints according to their uncertainties, and thus their systematic uncertainties are propagated into the statistical uncertainties reported on the physics parameters themselves. The systematic uncertainties for ϕ_s, $\Delta\Gamma_s$ and Γ_s can be treated as uncorrelated between this result and those in Ref. [2].

8. Conclusions

Using a dataset corresponding to an integrated luminosity of $3.0\,\text{fb}^{-1}$ collected by the LHCb experiment in pp collisions during LHC Run 1, a flavour tagged, decay-time dependent angular analysis of approximately 4700 $B_s^0 \to \psi(2S)\phi$ decays is performed. The analysis gives access to a number of physics parameters including the *CP*-violating phase, average decay-width and decay-width difference of the B_s^0 system as well as the polarisation amplitudes and strong phases of the decay. The effective decay-time resolution and effective tagging power are approximately 47 fs and 3.9%, respectively. This is the first measurement of the *CP* content of the $B_s^0 \to \psi(2S)\phi$ decay and first time that ϕ_s and $\Delta\Gamma_s$ have been measured in a final state containing the $\psi(2S)$ resonance. The results are consistent with previous measurements [2–6], the SM predictions [32–34], and show no evidence of *CP* violation in the interference between B_s^0 meson mixing and decay. The parameter $|\lambda|$ is consistent with unity, implying no evidence for direct *CP* violation in $B_s^0 \to \psi(2S)\phi$ decays. The fraction of longitudinal polarisation in the $B_s^0 \to \psi(2S)\phi$ decay is measured to be lower than that in the $B_s^0 \to J/\psi\phi$ decay, consistent with the predictions of Ref. [36].

Acknowledgements

We express our gratitude to our colleagues in the CERN accelerator departments for the excellent performance of the LHC. We thank the technical and administrative staff at the LHCb institutes. We acknowledge support from CERN and from the national agencies: CAPES, CNPq, FAPERJ and FINEP (Brazil); NSFC (China); CNRS/IN2P3 (France); BMBF, DFG and MPG (Germany); INFN (Italy); FOM and NWO (The Netherlands); MNiSW and NCN (Poland); MEN/IFA (Romania); MinES and FANO (Russia); MinECo (Spain); SNSF and SER (Switzerland); NASU (Ukraine); STFC (United Kingdom); NSF (USA). We acknowledge the computing resources that are provided by CERN, IN2P3 (France), KIT and DESY (Germany), INFN (Italy), SURF (The Netherlands), PIC (Spain), GridPP (United Kingdom), RRCKI and Yandex LLC (Russia), CSCS (Switzerland), IFIN-HH (Romania), CBPF (Brazil), PL-GRID (Poland) and OSC (USA). We are indebted to the communities behind the multiple open source software packages on which we depend. Individual groups or members have received support from AvH Foundation (Germany), EPLANET, Marie Skłodowska-Curie Actions and ERC (European Union), Conseil Général de Haute-Savoie, Labex ENIGMASS and OCEVU, Région Auvergne (France), RFBR and Yandex LLC (Russia), GVA, XuntaGal and GENCAT (Spain), Herchel Smith Fund, The Royal Society, Royal Commission for the Exhibition of 1851 and the Leverhulme Trust (United Kingdom).

References

[1] M. Kobayashi, T. Maskawa, CP violation in the renormalizable theory of weak interaction, Prog. Theor. Phys. 49 (1973) 652;
N. Cabibbo, Unitary symmetry and leptonic decays, Phys. Rev. Lett. 10 (1963) 531.

[2] LHCb collaboration, R. Aaij, et al., Precision measurement of *CP* violation in $B_s^0 \to J/\psi K^+K^-$ decays, Phys. Rev. Lett. 114 (2015) 041801, arXiv:1411.3104.

[3] D0 collaboration, V.M. Abazov, et al., Measurement of the *CP*-violating phase $\phi_s^{J/\psi\phi}$ using the flavor-tagged decay $B_s^0 \to J/\psi\phi$ in 8 fb^{-1} of $p\bar{p}$ collisions, Phys. Rev. D 85 (2012) 032006, arXiv:1109.3166.

[4] CDF collaboration, T. Aaltonen, et al., Measurement of the *CP*-violating phase $\beta_s^{J/\psi\phi}$ in $B_s^0 \to J/\psi\phi$ decays with the CDF II detector, Phys. Rev. D 85 (2012) 072002, arXiv:1112.1726.

[5] CMS collaboration, V. Khachatryan, et al., Measurement of the *CP*-violating weak phase ϕ_s and the decay width difference $\Delta\Gamma_s$ using the $B_s^0 \to J/\psi\phi(1020)$ decay channel in pp collisions at $\sqrt{s} = 8$ TeV, Phys. Lett. B 757 (2016) 97, arXiv:1507.07527.

[6] ATLAS collaboration, G. Aad, et al., Measurement of the *CP*-violating phase ϕ_s and the B_s^0 meson decay width difference with $B_s^0 \to J/\psi\phi$ decays in ATLAS, arXiv:1601.03297.

[7] Heavy Flavor Averaging Group, Y. Amhis, et al., Averages of b-hadron, c-hadron, and τ-lepton properties as of summer 2014, arXiv:1412.7515, updated results and plots available at http://www.slac.stanford.edu/xorg/hfag/.

[8] J. Charles, et al., Current status of the Standard Model CKM fit and constraints on $\Delta F = 2$ new physics, Phys. Rev. D 91 (7) (2015) 073007, arXiv:1501.05013.

[9] A.J. Buras, Flavour theory: 2009, PoS EPS-HEP2009 (2009) 024, arXiv:0910.1032.

[10] C.-W. Chiang, et al., New physics in $B_s^0 \to J/\psi\phi$: a general analysis, J. High Energy Phys. 04 (2010) 031, arXiv:0910.2929.

[11] LHCb collaboration, R. Aaij, et al., Measurement of *CP* violation and the B_s^0 meson decay width difference with $B_s^0 \to J/\psi K^+K^-$ and $B_s^0 \to J/\psi\pi^+\pi^-$ decays, Phys. Rev. D 87 (2013) 112010, arXiv:1304.2600.

[12] LHCb collaboration, R. Aaij, et al., Measurement of the flavour-specific *CP*-violating asymmetry a_{sl}^s in B_s^0 decays, Phys. Lett. B 728 (2014) 607, arXiv:1308.1048.

[13] LHCb collaboration, R. Aaij, et al., Measurement of the *CP* asymmetry in B_s^0–$\overline{B}_s^0$ mixing, Phys. Rev. Lett. 117 (2016) 061803, arXiv:1605.09768.

[14] LHCb collaboration, A.A. Alves Jr., et al., The LHCb detector at the LHC, J. Instrum. 3 (2008) S08005.

[15] LHCb collaboration, R. Aaij, et al., LHCb detector performance, Int. J. Mod. Phys. A 30 (2015) 1530022, arXiv:1412.6352.

[16] R. Aaij, et al., The LHCb trigger and its performance in 2011, J. Instrum. 8 (2013) P04022, arXiv:1211.3055.

[17] T. Sjöstrand, S. Mrenna, P. Skands, PYTHIA 6.4 physics and manual, J. High Energy Phys. 05 (2006) 026, arXiv:hep-ph/0603175;
T. Sjöstrand, S. Mrenna, P. Skands, A brief introduction to PYTHIA 8.1, Comput. Phys. Commun. 178 (2008) 852, arXiv:0710.3820.

[18] I. Belyaev, et al., Handling of the generation of primary events in Gauss, the LHCb simulation framework, J. Phys. Conf. Ser. 331 (2011) 032047.

[19] D.J. Lange, The EvtGen particle decay simulation package, Nucl. Instrum. Methods A 462 (2001) 152.

[20] P. Golonka, Z. Was, PHOTOS Monte Carlo: a precision tool for QED corrections in Z and W decays, Eur. Phys. J. C 45 (2006) 97, arXiv:hep-ph/0506026.

[21] Geant4 collaboration, J. Allison, et al., Geant4 developments and applications, IEEE Trans. Nucl. Sci. 53 (2006) 270;
Geant4 collaboration, S. Agostinelli, et al., Geant4: a simulation toolkit, Nucl. Instrum. Methods A 506 (2003) 250.

[22] M. Clemencic, et al., The LHCb simulation application, Gauss: design, evolution and experience, J. Phys. Conf. Ser. 331 (2011) 032023.

[23] Particle Data Group, K.A. Olive, et al., Review of particle physics, Chin. Phys. C 38 (2014) 090001, and 2015 update.

[24] W.D. Hulsbergen, Decay chain fitting with a Kalman filter, Nucl. Instrum. Methods A 552 (2005) 566, arXiv:physics/0503191.

[25] L. Breiman, J.H. Friedman, R.A. Olshen, C.J. Stone, Classification and Regression Trees, Wadsworth International Group, Belmont, California, USA, 1984.

[26] R.E. Schapire, Y. Freund, A decision-theoretic generalization of on-line learning and an application to boosting, J. Comput. Syst. Sci. 55 (1997) 119.

[27] T. Skwarnicki, A study of the radiative cascade transitions between the Upsilon-prime and Upsilon resonances, PhD thesis, Institute of Nuclear Physics, Krakow, 1986, DESY-F31-86-02.

[28] M. Pivk, F.R. Le Diberder, sPlot: a statistical tool to unfold data distributions, Nucl. Instrum. Methods A 555 (2005) 356, arXiv:physics/0402083.

[29] LHCb collaboration, R. Aaij, et al., Opposite-side flavour tagging of B mesons at the LHCb experiment, Eur. Phys. J. C 72 (2012) 2022, arXiv:1202.4979.

[30] LHCb collaboration, R. Aaij, et al., A new algorithm for identifying the flavour of B_s^0 mesons at LHCb, J. Instrum. 11 (2015) P05010, arXiv:1602.07252.

[31] LHCb collaboration, R. Aaij, et al., Determination of the sign of the decay width difference in the B_s^0 system, Phys. Rev. Lett. 108 (2012) 241801, arXiv:1202.4717.

[32] CKMfitter Group, J. Charles, et al., CP violation and the CKM matrix: assessing the impact of the asymmetric B factories, Eur. Phys. J. C 41 (2005) 1, arXiv:hep-ph/0406184.

[33] A. Lenz, U. Nierste, Theoretical update of B_s^0-$\overline{B}_s^0$ mixing, J. High Energy Phys. 06 (2007) 072, arXiv:hep-ph/0612167.

[34] M. Artuso, G. Borissov, A. Lenz, CP violation in the B_s^0 system, arXiv:1511.09466.

[35] LHCb collaboration, R. Aaij, et al., Angular analysis and differential branching fraction of the decay $B_s^0 \to \phi\mu^+\mu^-$, J. High Energy Phys. 09 (2015) 179, arXiv:1506.08777.

[36] G. Hiller, R. Zwicky, (A)symmetries of weak decays at and near the kinematic endpoint, J. High Energy Phys. 03 (2014) 042, arXiv:1312.1923.

LHCb Collaboration

R. Aaij[40], B. Adeva[39], M. Adinolfi[48], Z. Ajaltouni[5], S. Akar[6], J. Albrecht[10], F. Alessio[40], M. Alexander[53], S. Ali[43], G. Alkhazov[31], P. Alvarez Cartelle[55], A.A. Alves Jr[59], S. Amato[2], S. Amerio[23], Y. Amhis[7], L. An[41], L. Anderlini[18], G. Andreassi[41], M. Andreotti[17,g], J.E. Andrews[60], R.B. Appleby[56], O. Aquines Gutierrez[11], F. Archilli[43], P. d'Argent[12], J. Arnau Romeu[6], A. Artamonov[37], M. Artuso[61], E. Aslanides[6], G. Auriemma[26], M. Baalouch[5], I. Babuschkin[56], S. Bachmann[12], J.J. Back[50], A. Badalov[38], C. Baesso[62], S. Baker[55], W. Baldini[17], R.J. Barlow[56], C. Barschel[40], S. Barsuk[7], W. Barter[40], V. Batozskaya[29], B. Batsukh[61], V. Battista[41], A. Bay[41], L. Beaucourt[4], J. Beddow[53], F. Bedeschi[24], I. Bediaga[1], L.J. Bel[43], V. Bellee[41], N. Belloli[21,i], K. Belous[37], I. Belyaev[32], E. Ben-Haim[8], G. Bencivenni[19], S. Benson[40], J. Benton[48], A. Berezhnoy[33], R. Bernet[42], A. Bertolin[23], F. Betti[15], M.-O. Bettler[40], M. van Beuzekom[43], I. Bezshyiko[42], S. Bifani[47], P. Billoir[8], T. Bird[56], A. Birnkraut[10], A. Bitadze[56], A. Bizzeti[18,u], T. Blake[50], F. Blanc[41], J. Blouw[11], S. Blusk[61], V. Bocci[26], T. Boettcher[58], A. Bondar[36], N. Bondar[31,40], W. Bonivento[16], A. Borgheresi[21,i], S. Borghi[56], M. Borisyak[35], M. Borsato[39], F. Bossu[7], M. Boubdir[9], T.J.V. Bowcock[54], E. Bowen[42], C. Bozzi[17,40], S. Braun[12], M. Britsch[12], T. Britton[61], J. Brodzicka[56], E. Buchanan[48], C. Burr[56], A. Bursche[2], J. Buytaert[40], S. Cadeddu[16], R. Calabrese[17,g], M. Calvi[21,i], M. Calvo Gomez[38,m], A. Camboni[38], P. Campana[19], D. Campora Perez[40], D.H. Campora Perez[40], L. Capriotti[56], A. Carbone[15,e], G. Carboni[25,j], R. Cardinale[20,h], A. Cardini[16], P. Carniti[21,i], L. Carson[52], K. Carvalho Akiba[2], G. Casse[54], L. Cassina[21,i], L. Castillo Garcia[41], M. Cattaneo[40], Ch. Cauet[10], G. Cavallero[20], R. Cenci[24,t], M. Charles[8], Ph. Charpentier[40], G. Chatzikonstantinidis[47], M. Chefdeville[4], S. Chen[56], S.-F. Cheung[57], V. Chobanova[39], M. Chrzaszcz[42,27], X. Cid Vidal[39], G. Ciezarek[43], P.E.L. Clarke[52], M. Clemencic[40], H.V. Cliff[49], J. Closier[40], V. Coco[59], J. Cogan[6], E. Cogneras[5], V. Cogoni[16,40,f], L. Cojocariu[30], G. Collazuol[23,o], P. Collins[40], A. Comerma-Montells[12], A. Contu[40], A. Cook[48], S. Coquereau[8], G. Corti[40], M. Corvo[17,g], C.M. Costa Sobral[50], B. Couturier[40], G.A. Cowan[52,*], D.C. Craik[52], A. Crocombe[50], M. Cruz Torres[62], S. Cunliffe[55], R. Currie[55], C. D'Ambrosio[40], E. Dall'Occo[43], J. Dalseno[48], P.N.Y. David[43], A. Davis[59], O. De Aguiar Francisco[2], K. De Bruyn[6], S. De Capua[56], M. De Cian[12], J.M. De Miranda[1], L. De Paula[2], M. De Serio[14,d], P. De Simone[19], C.-T. Dean[53], D. Decamp[4], M. Deckenhoff[10], L. Del Buono[8], M. Demmer[10], D. Derkach[35], O. Deschamps[5], F. Dettori[40], B. Dey[22], A. Di Canto[40], H. Dijkstra[40], F. Dordei[40], M. Dorigo[41], A. Dosil Suárez[39], A. Dovbnya[45], K. Dreimanis[54], L. Dufour[43], G. Dujany[56], K. Dungs[40], P. Durante[40], R. Dzhelyadin[37], A. Dziurda[40], A. Dzyuba[31], N. Déléage[4], S. Easo[51], M. Ebert[52], U. Egede[55], V. Egorychev[32], S. Eidelman[36], S. Eisenhardt[52], U. Eitschberger[10], R. Ekelhof[10], L. Eklund[53], Ch. Elsasser[42], S. Ely[61], S. Esen[12], H.M. Evans[49], T. Evans[57], A. Falabella[15], N. Farley[47], S. Farry[54], R. Fay[54], D. Fazzini[21,i], D. Ferguson[52], V. Fernandez Albor[39], A. Fernandez Prieto[39], F. Ferrari[15,40],

F. Ferreira Rodrigues[1], M. Ferro-Luzzi[40], S. Filippov[34], R.A. Fini[14], M. Fiore[17,g], M. Fiorini[17,g], M. Firlej[28], C. Fitzpatrick[41], T. Fiutowski[28], F. Fleuret[7,b], K. Fohl[40], M. Fontana[16], F. Fontanelli[20,h], D.C. Forshaw[61], R. Forty[40], V. Franco Lima[54], M. Frank[40], C. Frei[40], J. Fu[22,q], E. Furfaro[25,j], C. Färber[40], A. Gallas Torreira[39], D. Galli[15,e], S. Gallorini[23], S. Gambetta[52], M. Gandelman[2], P. Gandini[57], Y. Gao[3], L.M. Garcia Martin[68], J. García Pardiñas[39], J. Garra Tico[49], L. Garrido[38], P.J. Garsed[49], D. Gascon[38], C. Gaspar[40], L. Gavardi[10], G. Gazzoni[5], D. Gerick[12], E. Gersabeck[12], M. Gersabeck[56], T. Gershon[50], Ph. Ghez[4], S. Gianì[41], V. Gibson[49], O.G. Girard[41], L. Giubega[30], K. Gizdov[52], V.V. Gligorov[8], D. Golubkov[32], A. Golutvin[55,40], A. Gomes[1,a], I.V. Gorelov[33], C. Gotti[21,i], M. Grabalosa Gándara[5], R. Graciani Diaz[38], L.A. Granado Cardoso[40], E. Graugés[38], E. Graverini[42], G. Graziani[18], A. Grecu[30], P. Griffith[47], L. Grillo[21], B.R. Gruberg Cazon[57], O. Grünberg[66], E. Gushchin[34], Yu. Guz[37], T. Gys[40], C. Göbel[62], T. Hadavizadeh[57], C. Hadjivasiliou[5], G. Haefeli[41], C. Haen[40], S.C. Haines[49], S. Hall[55], B. Hamilton[60], X. Han[12], S. Hansmann-Menzemer[12], N. Harnew[57], S.T. Harnew[48], J. Harrison[56], M. Hatch[40], J. He[63], T. Head[41], A. Heister[9], K. Hennessy[54], P. Henrard[5], L. Henry[8], J.A. Hernando Morata[39], E. van Herwijnen[40], M. Heß[66], A. Hicheur[2], D. Hill[57], C. Hombach[56], H. Hopchev[41], W. Hulsbergen[43], T. Humair[55], M. Hushchyn[35], N. Hussain[57], D. Hutchcroft[54], V. Iakovenko[46], M. Idzik[28], P. Ilten[58], R. Jacobsson[40], A. Jaeger[12], J. Jalocha[57], E. Jans[43], A. Jawahery[60], F. Jiang[3], M. John[57], D. Johnson[40], C.R. Jones[49], C. Joram[40], B. Jost[40], N. Jurik[61], S. Kandybei[45], W. Kanso[6], M. Karacson[40], J.M. Kariuki[48], S. Karodia[53], M. Kecke[12], M. Kelsey[61], I.R. Kenyon[47], M. Kenzie[40], T. Ketel[44], E. Khairullin[35], B. Khanji[21,40,i], C. Khurewathanakul[41], T. Kirn[9], S. Klaver[56], K. Klimaszewski[29], S. Koliiev[46], M. Kolpin[12], I. Komarov[41], R.F. Koopman[44], P. Koppenburg[43], A. Kozachuk[33], M. Kozeiha[5], L. Kravchuk[34], K. Kreplin[12], M. Kreps[50], P. Krokovny[36], F. Kruse[10], W. Krzemien[29], W. Kucewicz[27,l], M. Kucharczyk[27], V. Kudryavtsev[36], A.K. Kuonen[41], K. Kurek[29], T. Kvaratskheliya[32,40], D. Lacarrere[40], G. Lafferty[56,40], A. Lai[16], D. Lambert[52], G. Lanfranchi[19], C. Langenbruch[9], T. Latham[50], C. Lazzeroni[47], R. Le Gac[6], J. van Leerdam[43], J.-P. Lees[4], A. Leflat[33,40], J. Lefrançois[7], R. Lefèvre[5], F. Lemaitre[40], E. Lemos Cid[39], O. Leroy[6], T. Lesiak[27], B. Leverington[12], Y. Li[7], T. Likhomanenko[35,67], R. Lindner[40], C. Linn[40], F. Lionetto[42], B. Liu[16], X. Liu[3], D. Loh[50], I. Longstaff[53], J.H. Lopes[2], D. Lucchesi[23,o], M. Lucio Martinez[39], H. Luo[52], A. Lupato[23], E. Luppi[17,g], O. Lupton[57], A. Lusiani[24], X. Lyu[63], F. Machefert[7], F. Maciuc[30], O. Maev[31], K. Maguire[56], S. Malde[57], A. Malinin[67], T. Maltsev[36], G. Manca[7], G. Mancinelli[6], P. Manning[61], J. Maratas[5,v], J.F. Marchand[4], U. Marconi[15], C. Marin Benito[38], P. Marino[24,t], J. Marks[12], G. Martellotti[26], M. Martin[6], M. Martinelli[41], D. Martinez Santos[39], F. Martinez Vidal[68], D. Martins Tostes[2], L.M. Massacrier[7], A. Massafferri[1], R. Matev[40], A. Mathad[50], Z. Mathe[40], C. Matteuzzi[21], A. Mauri[42], B. Maurin[41], A. Mazurov[47], M. McCann[55], J. McCarthy[47], A. McNab[56], R. McNulty[13], B. Meadows[59], F. Meier[10], M. Meissner[12], D. Melnychuk[29], M. Merk[43], A. Merli[22,q], E. Michielin[23], D.A. Milanes[65], M.-N. Minard[4], D.S. Mitzel[12], A. Mogini[8], J. Molina Rodriguez[62], I.A. Monroy[65], S. Monteil[5], M. Morandin[23], P. Morawski[28], A. Mordà[6], M.J. Morello[24,t], J. Moron[28], A.B. Morris[52], R. Mountain[61], F. Muheim[52], M. Mulder[43], M. Mussini[15], D. Müller[56], J. Müller[10], K. Müller[42], V. Müller[10], P. Naik[48], T. Nakada[41], R. Nandakumar[51], A. Nandi[57], I. Nasteva[2], M. Needham[52], N. Neri[22], S. Neubert[12], N. Neufeld[40], M. Neuner[12], A.D. Nguyen[41], C. Nguyen-Mau[41,n], S. Nieswand[9], R. Niet[10], N. Nikitin[33], T. Nikodem[12], A. Novoselov[37], D.P. O'Hanlon[50], A. Oblakowska-Mucha[28], V. Obraztsov[37], S. Ogilvy[19], R. Oldeman[49], C.J.G. Onderwater[69], J.M. Otalora Goicochea[2], A. Otto[40], P. Owen[42], A. Oyanguren[68], P.R. Pais[41], A. Palano[14,d], F. Palombo[22,q], M. Palutan[19], J. Panman[40], A. Papanestis[51], M. Pappagallo[14,d], L.L. Pappalardo[17,g], W. Parker[60], C. Parkes[56], G. Passaleva[18], A. Pastore[14,d], G.D. Patel[54], M. Patel[55], C. Patrignani[15,e], A. Pearce[56,51], A. Pellegrino[43], G. Penso[26], M. Pepe Altarelli[40], S. Perazzini[40], P. Perret[5], L. Pescatore[47], K. Petridis[48], A. Petrolini[20,h], A. Petrov[67], M. Petruzzo[22,q], E. Picatoste Olloqui[38], B. Pietrzyk[4], M. Pikies[27], D. Pinci[26], A. Pistone[20], A. Piucci[12], S. Playfer[52], M. Plo Casasus[39], T. Poikela[40], F. Polci[8], A. Poluektov[50,36], I. Polyakov[61], E. Polycarpo[2], G.J. Pomery[48], A. Popov[37], D. Popov[11,40], B. Popovici[30], S. Poslavskii[37], C. Potterat[2], E. Price[48], J.D. Price[54], J. Prisciandaro[39], A. Pritchard[54], C. Prouve[48], V. Pugatch[46], A. Puig Navarro[41], G. Punzi[24,p], W. Qian[57], R. Quagliani[7,48], B. Rachwal[27], J.H. Rademacker[48], M. Rama[24], M. Ramos Pernas[39], M.S. Rangel[2], I. Raniuk[45], G. Raven[44], F. Redi[55], S. Reichert[10], A.C. dos Reis[1], C. Remon Alepuz[68], V. Renaudin[7], S. Ricciardi[51], S. Richards[48], M. Rihl[40], K. Rinnert[54,40], V. Rives Molina[38], P. Robbe[7,40], A.B. Rodrigues[1],

E. Rodrigues[59], J.A. Rodriguez Lopez[65], P. Rodriguez Perez[56], A. Rogozhnikov[35], S. Roiser[40], V. Romanovskiy[37], A. Romero Vidal[39], J.W. Ronayne[13], M. Rotondo[19], M.S. Rudolph[61], T. Ruf[40], P. Ruiz Valls[68], J.J. Saborido Silva[39], E. Sadykhov[32], N. Sagidova[31], B. Saitta[16,f], V. Salustino Guimaraes[2], C. Sanchez Mayordomo[68], B. Sanmartin Sedes[39], R. Santacesaria[26], C. Santamarina Rios[39], M. Santimaria[19], E. Santovetti[25,j], A. Sarti[19,k], C. Satriano[26,s], A. Satta[25], D.M. Saunders[48], D. Savrina[32,33], S. Schael[9], M. Schellenberg[10], M. Schiller[40], H. Schindler[40], M. Schlupp[10], M. Schmelling[11], T. Schmelzer[10], B. Schmidt[40], O. Schneider[41], A. Schopper[40], K. Schubert[10], M. Schubiger[41], M.-H. Schune[7], R. Schwemmer[40], B. Sciascia[19], A. Sciubba[26,k], A. Semennikov[32], A. Sergi[47], N. Serra[42], J. Serrano[6], L. Sestini[23], P. Seyfert[21], M. Shapkin[37], I. Shapoval[17,45,g], Y. Shcheglov[31], T. Shears[54], L. Shekhtman[36], V. Shevchenko[67], A. Shires[10], B.G. Siddi[17], R. Silva Coutinho[42], L. Silva de Oliveira[2], G. Simi[23,o], S. Simone[14,d], M. Sirendi[49], N. Skidmore[48], T. Skwarnicki[61], E. Smith[55], I.T. Smith[52], J. Smith[49], M. Smith[55], H. Snoek[43], M.D. Sokoloff[59], F.J.P. Soler[53], D. Souza[48], B. Souza De Paula[2], B. Spaan[10], P. Spradlin[53], S. Sridharan[40], F. Stagni[40], M. Stahl[12], S. Stahl[40], P. Stefko[41], S. Stefkova[55], O. Steinkamp[42], S. Stemmle[12], O. Stenyakin[37], S. Stevenson[57], S. Stoica[30], S. Stone[61], B. Storaci[42], S. Stracka[24,t], M. Straticiuc[30], U. Straumann[42], L. Sun[59], W. Sutcliffe[55], K. Swientek[28], V. Syropoulos[44], M. Szczekowski[29], T. Szumlak[28], S. T'Jampens[4], A. Tayduganov[6], T. Tekampe[10], G. Tellarini[17,g], F. Teubert[40], C. Thomas[57], E. Thomas[40], J. van Tilburg[43], M.J. Tilley[55], V. Tisserand[4], M. Tobin[41], S. Tolk[49], L. Tomassetti[17,g], D. Tonelli[40], S. Topp-Joergensen[57], F. Toriello[61], E. Tournefier[4], S. Tourneur[41], K. Trabelsi[41], M. Traill[53], M.T. Tran[41], M. Tresch[42], A. Trisovic[40], A. Tsaregorodtsev[6], P. Tsopelas[43], A. Tully[49], N. Tuning[43], A. Ukleja[29], A. Ustyuzhanin[35,67], U. Uwer[12], C. Vacca[16,40,f], V. Vagnoni[15,40], S. Valat[40], G. Valenti[15], A. Vallier[7], R. Vazquez Gomez[19], P. Vazquez Regueiro[39], S. Vecchi[17], M. van Veghel[43], J.J. Velthuis[48], M. Veltri[18,r], G. Veneziano[41], A. Venkateswaran[61], M. Vernet[5], M. Vesterinen[12], B. Viaud[7], D. Vieira[1], M. Vieites Diaz[39], X. Vilasis-Cardona[38,m], V. Volkov[33], A. Vollhardt[42], B. Voneki[40], D. Voong[48], A. Vorobyev[31], V. Vorobyev[36], C. Voß[66], J.A. de Vries[43], C. Vázquez Sierra[39], R. Waldi[66], C. Wallace[50], R. Wallace[13], J. Walsh[24], J. Wang[61], D.R. Ward[49], H.M. Wark[54], N.K. Watson[47], D. Websdale[55], A. Weiden[42], M. Whitehead[40], J. Wicht[50], G. Wilkinson[57,40], M. Wilkinson[61], M. Williams[40], M.P. Williams[47], M. Williams[58], T. Williams[47], F.F. Wilson[51], J. Wimberley[60], J. Wishahi[10], W. Wislicki[29], M. Witek[27], G. Wormser[7], S.A. Wotton[49], K. Wraight[53], S. Wright[49], K. Wyllie[40], Y. Xie[64], Z. Xing[61], Z. Xu[41], Z. Yang[3], H. Yin[64], J. Yu[64], X. Yuan[36], O. Yushchenko[37], M. Zangoli[15], K.A. Zarebski[47], M. Zavertyaev[11,c], L. Zhang[3], Y. Zhang[7], Y. Zhang[63], A. Zhelezov[12], Y. Zheng[63], A. Zhokhov[32], X. Zhu[3], V. Zhukov[9], S. Zucchelli[15]

[1] Centro Brasileiro de Pesquisas Físicas (CBPF), Rio de Janeiro, Brazil
[2] Universidade Federal do Rio de Janeiro (UFRJ), Rio de Janeiro, Brazil
[3] Center for High Energy Physics, Tsinghua University, Beijing, China
[4] LAPP, Université Savoie Mont-Blanc, CNRS/IN2P3, Annecy-Le-Vieux, France
[5] Clermont Université, Université Blaise Pascal, CNRS/IN2P3, LPC, Clermont-Ferrand, France
[6] CPPM, Aix-Marseille Université, CNRS/IN2P3, Marseille, France
[7] LAL, Université Paris-Sud, CNRS/IN2P3, Orsay, France
[8] LPNHE, Université Pierre et Marie Curie, Université Paris Diderot, CNRS/IN2P3, Paris, France
[9] I. Physikalisches Institut, RWTH Aachen University, Aachen, Germany
[10] Fakultät Physik, Technische Universität Dortmund, Dortmund, Germany
[11] Max-Planck-Institut für Kernphysik (MPIK), Heidelberg, Germany
[12] Physikalisches Institut, Ruprecht-Karls-Universität Heidelberg, Heidelberg, Germany
[13] School of Physics, University College Dublin, Dublin, Ireland
[14] Sezione INFN di Bari, Bari, Italy
[15] Sezione INFN di Bologna, Bologna, Italy
[16] Sezione INFN di Cagliari, Cagliari, Italy
[17] Sezione INFN di Ferrara, Ferrara, Italy
[18] Sezione INFN di Firenze, Firenze, Italy
[19] Laboratori Nazionali dell'INFN di Frascati, Frascati, Italy
[20] Sezione INFN di Genova, Genova, Italy
[21] Sezione INFN di Milano Bicocca, Milano, Italy
[22] Sezione INFN di Milano, Milano, Italy
[23] Sezione INFN di Padova, Padova, Italy
[24] Sezione INFN di Pisa, Pisa, Italy
[25] Sezione INFN di Roma Tor Vergata, Roma, Italy
[26] Sezione INFN di Roma La Sapienza, Roma, Italy
[27] Henryk Niewodniczanski Institute of Nuclear Physics Polish Academy of Sciences, Kraków, Poland
[28] AGH – University of Science and Technology, Faculty of Physics and Applied Computer Science, Kraków, Poland
[29] National Center for Nuclear Research (NCBJ), Warsaw, Poland
[30] Horia Hulubei National Institute of Physics and Nuclear Engineering, Bucharest-Magurele, Romania

[31] *Petersburg Nuclear Physics Institute (PNPI), Gatchina, Russia*
[32] *Institute of Theoretical and Experimental Physics (ITEP), Moscow, Russia*
[33] *Institute of Nuclear Physics, Moscow State University (SINP MSU), Moscow, Russia*
[34] *Institute for Nuclear Research of the Russian Academy of Sciences (INR RAN), Moscow, Russia*
[35] *Yandex School of Data Analysis, Moscow, Russia*
[36] *Budker Institute of Nuclear Physics (SB RAS) and Novosibirsk State University, Novosibirsk, Russia*
[37] *Institute for High Energy Physics (IHEP), Protvino, Russia*
[38] *ICCUB, Universitat de Barcelona, Barcelona, Spain*
[39] *Universidad de Santiago de Compostela, Santiago de Compostela, Spain*
[40] *European Organization for Nuclear Research (CERN), Geneva, Switzerland*
[41] *Ecole Polytechnique Fédérale de Lausanne (EPFL), Lausanne, Switzerland*
[42] *Physik-Institut, Universität Zürich, Zürich, Switzerland*
[43] *Nikhef National Institute for Subatomic Physics, Amsterdam, The Netherlands*
[44] *Nikhef National Institute for Subatomic Physics and VU University Amsterdam, Amsterdam, The Netherlands*
[45] *NSC Kharkiv Institute of Physics and Technology (NSC KIPT), Kharkiv, Ukraine*
[46] *Institute for Nuclear Research of the National Academy of Sciences (KINR), Kyiv, Ukraine*
[47] *University of Birmingham, Birmingham, United Kingdom*
[48] *H.H. Wills Physics Laboratory, University of Bristol, Bristol, United Kingdom*
[49] *Cavendish Laboratory, University of Cambridge, Cambridge, United Kingdom*
[50] *Department of Physics, University of Warwick, Coventry, United Kingdom*
[51] *STFC Rutherford Appleton Laboratory, Didcot, United Kingdom*
[52] *School of Physics and Astronomy, University of Edinburgh, Edinburgh, United Kingdom*
[53] *School of Physics and Astronomy, University of Glasgow, Glasgow, United Kingdom*
[54] *Oliver Lodge Laboratory, University of Liverpool, Liverpool, United Kingdom*
[55] *Imperial College London, London, United Kingdom*
[56] *School of Physics and Astronomy, University of Manchester, Manchester, United Kingdom*
[57] *Department of Physics, University of Oxford, Oxford, United Kingdom*
[58] *Massachusetts Institute of Technology, Cambridge, MA, United States*
[59] *University of Cincinnati, Cincinnati, OH, United States*
[60] *University of Maryland, College Park, MD, United States*
[61] *Syracuse University, Syracuse, NY, United States*
[62] *Pontifícia Universidade Católica do Rio de Janeiro (PUC-Rio), Rio de Janeiro, Brazil* [w]
[63] *University of Chinese Academy of Sciences, Beijing, China* [x]
[64] *Institute of Particle Physics, Central China Normal University, Wuhan, Hubei, China* [x]
[65] *Departamento de Fisica, Universidad Nacional de Colombia, Bogota, Colombia* [y]
[66] *Institut für Physik, Universität Rostock, Rostock, Germany* [z]
[67] *National Research Centre Kurchatov Institute, Moscow, Russia* [aa]
[68] *Instituto de Fisica Corpuscular (IFIC), Universitat de Valencia-CSIC, Valencia, Spain* [ab]
[69] *Van Swinderen Institute, University of Groningen, Groningen, The Netherlands* [ac]

[*] Corresponding author.
E-mail address: greig.cowan@cern.ch (G.A. Cowan).

[a] Universidade Federal do Triângulo Mineiro (UFTM), Uberaba-MG, Brazil.
[b] Laboratoire Leprince-Ringuet, Palaiseau, France.
[c] P.N. Lebedev Physical Institute, Russian Academy of Science (LPI RAS), Moscow, Russia.
[d] Università di Bari, Bari, Italy.
[e] Università di Bologna, Bologna, Italy.
[f] Università di Cagliari, Cagliari, Italy.
[g] Università di Ferrara, Ferrara, Italy.
[h] Università di Genova, Genova, Italy.
[i] Università di Milano Bicocca, Milano, Italy.
[j] Università di Roma Tor Vergata, Roma, Italy.
[k] Università di Roma La Sapienza, Roma, Italy.
[l] AGH – University of Science and Technology, Faculty of Computer Science, Electronics and Telecommunications, Kraków, Poland.
[m] LIFAELS, La Salle, Universitat Ramon Llull, Barcelona, Spain.
[n] Hanoi University of Science, Hanoi, Viet Nam.
[o] Università di Padova, Padova, Italy.
[p] Università di Pisa, Pisa, Italy.
[q] Università degli Studi di Milano, Milano, Italy.
[r] Università di Urbino, Urbino, Italy.
[s] Università della Basilicata, Potenza, Italy.
[t] Scuola Normale Superiore, Pisa, Italy.
[u] Università di Modena e Reggio Emilia, Modena, Italy.
[v] Iligan Institute of Technology (IIT), Iligan, Philippines.
[w] Associated to Universidade Federal do Rio de Janeiro (UFRJ), Rio de Janeiro, Brazil.
[x] Associated to Center for High Energy Physics, Tsinghua University, Beijing, China.
[y] Associated to LPNHE, Université Pierre et Marie Curie, Université Paris Diderot, CNRS/IN2P3, Paris, France.
[z] Associated to Physikalisches Institut, Ruprecht-Karls-Universität Heidelberg, Heidelberg, Germany.
[aa] Associated to Institute of Theoretical and Experimental Physics (ITEP), Moscow, Russia.
[ab] Associated to ICCUB, Universitat de Barcelona, Barcelona, Spain.
[ac] Associated to Nikhef National Institute for Subatomic Physics, Amsterdam, The Netherlands.